Time reversal beamforming for powering ultrasonic implants

Braeden C. Benedict[1], Mohammad Meraj Ghanbari[2], Sina Faraji Alamouti[2], Nathan Tessema Ersumo[1], and Rikky Muller[1,2,3]

***Abstract*— Efficient ultrasonic beamforming to millimeter-scale neural implants can reduce implant volume, improve tolerance to misalignment, and allow multiple implants to be operated simultaneously. This work proposes the use of time reversal, a computationally simple approach to beamforming that is robust despite scattering and inhomogeneity of the acoustic medium. A custom ultrasound phased array system is used to demonstrate beam focusing and steering both in a liquid phantom and through tissue. Time reversal is experimentally compared with other beamforming techniques by measuring energy transfer efficiency at varying depths and angles. Simultaneous power delivery to multiple implants is also demonstrated.**

I. INTRODUCTION

Wireless millimeter-scale implants are attractive due to their minimal invasiveness and untethered operation, and they have been proposed for a range of peripheral nerve recording and stimulation applications [1]–[3]. Ultrasound (US) has emerged as a promising power delivery and communication modality for deep-tissue implants. When compared with electromagnetic waves, US offers efficient propagation in tissue and a relatively small wavelength, which enable the use of millimeter and sub-millimeter scale acoustic resonators implanted in deep tissue [1], [4]. Such an US implant includes a piezoceramic resonator (piezo), an integrated circuit, and optionally an energy storage capacitor. An external transducer provides US energy which is harvested by the piezo. The implant communicates with the external transducer (which also functions as a receiver) either by actively driving its piezo or by modulating the backscattered signal amplitude [3]. Piezo volume (a large percentage of total implant volume) determines the harvestable power for a given US intensity [5]; therefore, efficient delivery of power to the implant allows for reduction of the implant volume.

A single-element focused or unfocused external transducer is used with most published US implants. A focused transducer provides greater link efficiency for high power applications such as neural stimulation, but this setup can tolerate only a few millimeters misalignment [1], [2]. While multiple implants could be powered if placed in close proximity to one another, it is preferable to record or stimulate at multiple locations. To overcome these limitations, a transducer array can be used to dynamically focus and steer US energy by manipulating the phase at each element. Linear phased arrays (Nx1 elements) are used in ultrasound imaging to sweep the beam over a cross-sectional plane, and several have been demonstrated for power delivery to US implants [6]–[8]. In this work we fabricated a planar array (NxM elements) to allow for steering to locations within a 3D volume of tissue.

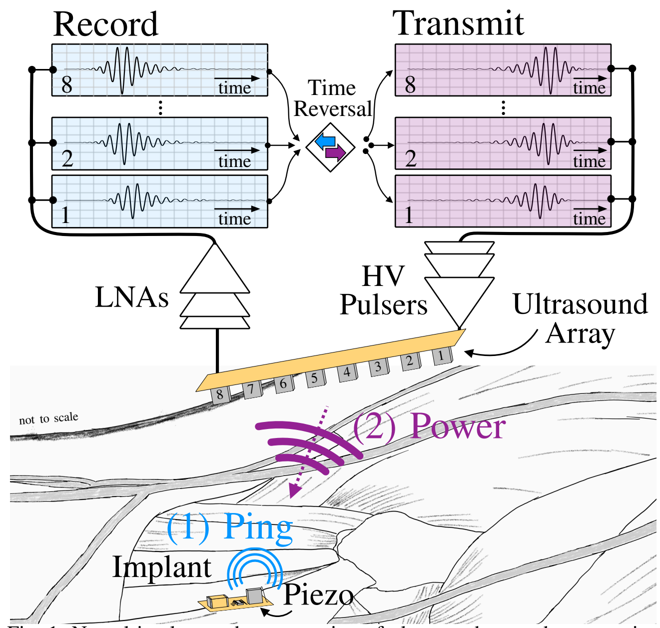

Fig. 1: Neural implant and cross-section of ultrasound array demonstrating the concept of time reversal.

In its simplest implementation, transmit beamforming can be achieved by calculating a time delay for each array element based on the differences of the distances from each element to the implant and the propagation speed in the medium [6]. This requires prior knowledge of the target implant position relative to the array. To localize the implant, a subset of array elements can record either a pulse sent by the implant or a backscattered signal received from the implant [8], [9]. Time delays can be calculated by finding the maximum of the cross-correlation between signals received on the individual array elements. The location of the implant can then be found by solving a nonlinear optimization problem [8]. Once the location is determined, the time delay beamforming method can be applied. This does not account for tissue inhomogeneity and scattering which may distort and redirect the beam. In contrast, this work proposes the use of a computationally simple method for ultrasonic beamforming to neural implants that is inherently robust to tissue inhomogeneity and scattering.

Research supported by the National Science Foundation Graduate Research Fellowship Program, the sponsors of the Berkeley Wireless Research Center, the Hellman Fellows Fund, and The Weill Neurohub.

[1]B.C.B., N.T.E., and R.M. are with UC Berkeley/UC San Francisco Joint Program in Bioengineering, Berkeley, CA, 94720 USA. braeden@berkeley.edu

[2]M.M.G., S.F.A., and R.M. are with the Department of Electrical Engineering and Computer Sciences, University of California, Berkeley, Berkeley, CA 94720, USA.

[3]R.M. is with Chan Zuckerberg Biohub, San Francisco, CA, 94158, USA.

II. Time Reversal

Time reversal (TR) beamforming requires no prior knowledge of the implant position or characteristics of the medium. In a lossless medium, time reversal US beamforming has been shown to be the optimal solution for maximizing pressure at a target [10]. In such a medium, the position and time-varying pressure field $P(\vec{r},t)$ is described by:

$$\vec{\nabla}\cdot\left(\frac{\vec{\nabla}P}{\rho}\right)-\frac{1}{\rho c^2}\frac{\partial^2 P}{\partial t^2}=0. \tag{1}$$

The space-varying propagation speed and density are given by $c(\vec{r})$ and $\rho(\vec{r})$, respectively. Since there is only a second-order time derivative, if $P(\vec{r},t)$ is a solution then $P(\vec{r},-t)$ must also be a solution. With an additional attenuation term this property is lost, but since attenuation is low in biological tissue this remains a valid approximation [10]. Even in cases with significant attenuation, such as focusing through the skull, a modified time reversal procedure can be used [11].

An illustration of the time reversal process is shown in Fig. 1. The implant sends out an acoustic pulse or "ping" received by the ultrasound array. These signals are recorded from the array elements, reversed in time, and played back to focus acoustic power on the targeted implant. This procedure could be repeated intermittently to correct for the implant shifting relative to the array. To initially power up the implant before the ping, the external ultrasound array would start in a high-power mode and/or sweep its focus using standard time delay beamforming. After the time reversal procedure, the external transducer power would be lowered since power could now be efficiently delivered to the implant. This protocol assumes the implant can actively drive the piezo; an alternate iterative pulse-echo time reversal sequence is possible if the implant communicates only through backscatter [11].

Finally, there is a distinction between true time reversal and using a signal from the implant to calculate the required time/phase shifts between elements [9], which we also demonstrate and refer to as phase reversal. This approach is a specific case of time reversal in which the received signals are perfectly sinusoidal, and it allows for continuous beamforming. However, in a heterogenous, highly scattering medium, the received signals will not be sinusoidal [12]. Time reversal will still work in these conditions, but it only provides pulses of finite length. This is well-suited for powering US implants since they are placed in inhomogeneous tissue and typically receive transient pulses of power.

III. Methods

A. Array Fabrication

The 52-element, 13 mm diameter planar array was assembled on a 0.3 mm polyimide flexible printed circuit board. Lead zirconate titanate piezoceramic (APC851) was diced into 0.8 mm cubes, and these elements were attached with silver epoxy (EPO-TEK H20E). The top ground electrodes were connected using bonding wire and silver epoxy. An image of the array is included in Fig. 2. Additional backing and matching layers can be added to improve efficiency and protect the elements [13]. Impedance measurements

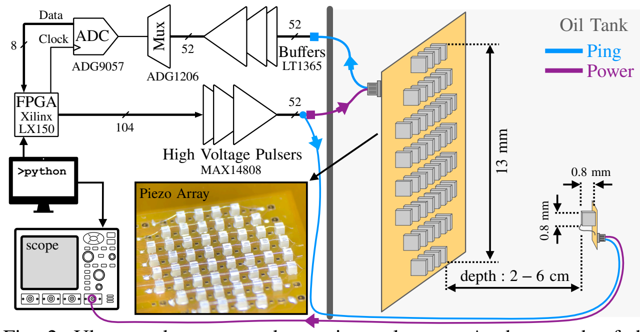

Fig. 2: Ultrasound system and experimental setup. A photograph of the piezo array is also shown.

revealed only 4 defective elements; the remainder showed good matching with each other and with finite element model simulations [5]. At the series resonant frequency of 1.5 MHz (used for all measurements), the piezos can be modeled as a Thevenin voltage source and purely real impedance, R_{Thev} = 4 kΩ.

To eliminate grating lobes, which degrade the efficiency of the array, a pitch is typically chosen between the wavelength λ (1.0 mm here) and $\lambda/2$, depending on the desired maximum steering angle. However, due to fabrication limitations a pitch of 1.8 mm was used; this should produce grating lobes at 33° and 51° from the axis when focused at 0° [14].

B. System Design

The custom US system (Fig. 2) incorporates 52 pulser channels (Maxim, MAX14808) controlled by an FPGA (Xilinx Spartan-6 LX150) clocked at 40 MHz. In power/transmit mode (Fig. 2, purple), the pulsers drive the array elements at ±3.3 V from a ±5 V supply (1.7 V diode drop), resulting in approximately 1.4 mW consumed by each element. The position of a 0.8 mm cube "implant" piezo in the oil medium is controlled by motorized translation stages (Thorlabs MTS50), and its open-circuit voltage is recorded using an oscilloscope and differential probe (Keysight N2750A).

In ping/receive mode (Fig. 2, blue), the implant piezo is driven by an US pulser for ten cycles at 1.5 MHz. Op amps (LT1365) are located close to the array board to buffer and amplify the received signals. These buffered signals are multiplexed to a single 8-bit analog to digital converter (ADC) (ADG9057), and the 40 MHz digitized signals are transferred to a PC. Recording from the entire array thus requires 52 identical pulses to be sent from the implant piezo; in a full implementation, these pulses could be synced based on a command sent from the array to the implant.

C. Signal Processing

After being transferred to the PC, the recorded signals from the ping are bandpass filtered and reversed in time. Signals are rescaled by the maximum value for each channel and quantized for the 3-level (-V_{High}, 0, +V_{High}) US pulsers. This could be implemented with simple digital processing and memory on-chip. The use of 3-level drive results in quantization error between the ideal time reversed pulse and the actual transmitted pulse. Finite element model simulations

(COMSOL Multiphysics) showed a 10% efficiency improvement was possible using 9-level ($\approx$ 3-bit) quantization when focusing at 0° in a homogeneous medium.

As a comparison to time reversal, phase reversal is also used. Here, the implant is driven for a single cycle, and the phase offsets between the signals received on the array are calculated by finding the maximum of the cross-correlation between the signals. These phase offsets are reversed and used to generate the waveforms for each array element. Finally, time delay beamforming is also used to target the implant using its known position.

Transmitted energy from the array is calculated from applied voltage and element impedance. Available received energy at the implant is calculated for a matched load (2.2 kΩ) for the piezo at resonance. Energy transfer efficiency is found by dividing received energy by transmitted energy. Efficiency is used to compare methods because the applied voltage waveforms and therefore input energy for time reversal are not explicitly controlled. To ensure a fair comparison, the number of cycles used for other methods is set to yield approximately equal input energy as time reversal.

IV. RESULTS

A. Acoustic Field Characterization

Energy transfer efficiency for a cross-section of the acoustic field when focusing at -10° is shown (Fig. 3). This was characterized in the homogeneous oil medium (c $\approx$ 1470 m/s, $\rho \approx 910$ kg/cm^3, $\alpha \approx 0.15$ dB/cm) at a depth of 5 cm and through 2.5 cm of porcine muscle tissue (c $\approx$ 1580 m/s, $\rho \approx 1070$ kg/cm^3, $\alpha \approx 2$ dB/cm) suspended in the oil medium at a total depth of 5 cm. Attenuation was greater through tissue, but the half-power beamwidth in both cases was 3.8° (3.3 mm diameter at 5 cm depth), which is consistent with the 3.7° theoretical beamwidth for this array [14].

Time reversal resulted in the highest peak efficiency, while phase reversal resulted in 83% and 77% efficiency when compared to time reversal in oil and tissue, respectively. Phase reversal was similar to time reversal since the porcine tissue was still a fairly homogeneous medium and the US pulsers only had 3-level drive. However, phase reversal required greater computational complexity. Efficiency using calculated time delays was approximately 65% compared to time reversal and required knowledge of the implant position.

Steering to -10° allowed for measurement of a predicted grating lobe resulting from the array pitch. When focusing on a target at 0° at 5 cm depth, the peak-to-peak voltage at the focal point in oil was 0.95 V, which results in 13 μW available power for the implant with only a $\pm$5 V supply for the phased array system. Efficiency can be improved by using arrays with more elements at a finer pitch to eliminate grating lobes. Excellent power transfer efficiency has been demonstrated for a 32-element linear (1D) array [7]; however, planar (2D) arrays allow for beamsteering in a 3D tissue volume. This work is meant as a self-comparison between beamforming methods that can be used with any planar or linear ultrasound array.

B. Beam Steering and Focusing

The ability to steer and focus on targets at varying angles and depths is shown in Fig. 4. Time and phase reversal were performed at each point. As a comparison, results with time delay beamforming using the known implant location and without beamforming are also shown. Efficiency drops off at larger steering angles due to increased beamwidth and increased angular misalignment that results from fixed implant orientation. Time reversal had 10 – 20% greater efficiency than phase reversal across all angles, and both

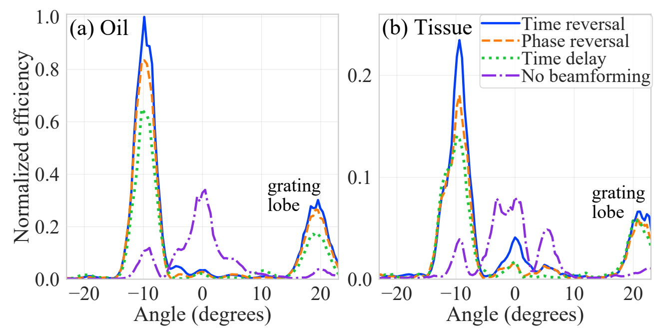

Fig. 3: Efficiency (normalized to peak time reversal measurement) as a function of angle when focused to -10° through (a) the homogeneous oil medium and (b) 2.5 cm porcine tissue suspended in the oil medium. Note the rescaled y-axis in (b) due to greater attenuation through tissue. Measurements taken at 5 cm depth.

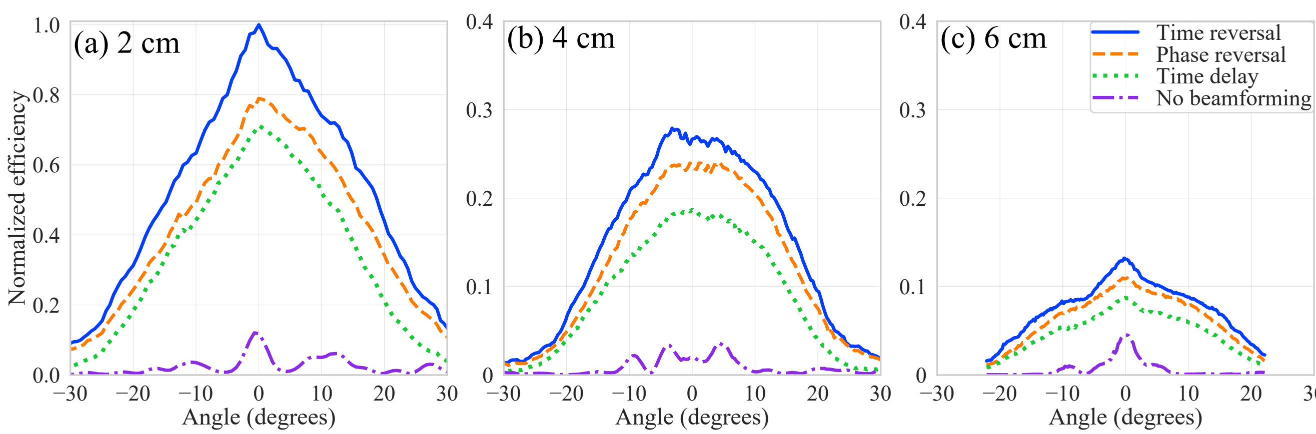

Fig. 4: Efficiency vs beamforming angle (normalized to peak time reversal measurement at 2 cm) when focusing at each position using time reversal, phase reversal, and time delay beamforming. Measurements were taken at depth planes of (a) 2 cm, (b) 4 cm, and (c) 6 cm. Measured angles were smaller in (c) due to limited translation stage travel. Note the rescaled y-axis in (b) and (c).

methods performed better than time delay beamforming, especially at larger angles. All methods improved efficiency compared to the unfocused array, with a 2.5x to 100x improvement using time reversal depending on position.

C. Multiple Implants

An advantage of a phased array system compared to a single-element transducer is the possibility of powering and communicating with multiple implants in different locations. This can occur one at a time using time-division multiplexing or simultaneously using techniques such as code-division multiple access [3], [15]. In the latter case, all implants must receive sufficient power to operate simultaneously. A previously demonstrated approach to powering multiple implants simultaneously was to partition the array and use half to target each implant [7]. In this work, the principle of superposition was used to simultaneously target multiple implants by playing back the sum of the time-reversed signals from each implant.

Two implants at 5 cm depth were powered separately (Fig. 5a,b), together using a partitioned array (Fig. 5c), and together using superposition (Fig. 5d). Time reversal was used to generate the transmitted waveforms. Superposition resulted in 0.6x and 0.43x efficiency at the targeted implants compared to powering each implant separately. This was expected since the acoustic energy was split between two foci and a perfect superposition was not possible due to pulser quantization. The partitioned array suffered from increased beamwidth due to the reduced aperture of each sub-array, resulting in 0.33x and 0.21x efficiency at each implant.

Table I shows the results from simultaneous time reversal focusing on two implants at different depths (3 and 4 cm). Superposition performed better than the partitioned array.

V. SUMMARY

In this work, we proposed and demonstrated the use of time reversal beamforming for ultrasonic power delivery to neural implants. We implemented this using a custom planar phased array, but the method can be used with any 1D or 2D ultrasound array. To our knowledge, this is the first demonstration of power delivery to implants using time reversal, a computationally simple yet theoretically optimal method for focusing and steering ultrasound through inhomogeneous media. Time reversal was 10 – 20% more efficient than phase reversal, the next best method. It was also 30 – 300% more efficient than time delay beamforming across the implant locations tested.

To the best of our knowledge, this is also the first work to use superposition to simultaneously power multiple implants, and this was shown to be up to twice as efficient as using half the array to power each implant. The eventual development of a compact phased array system with simple on-chip processing for time reversal beamforming would greatly improve the feasibility of powering a network of miniaturized implants for neural recording and stimulation.

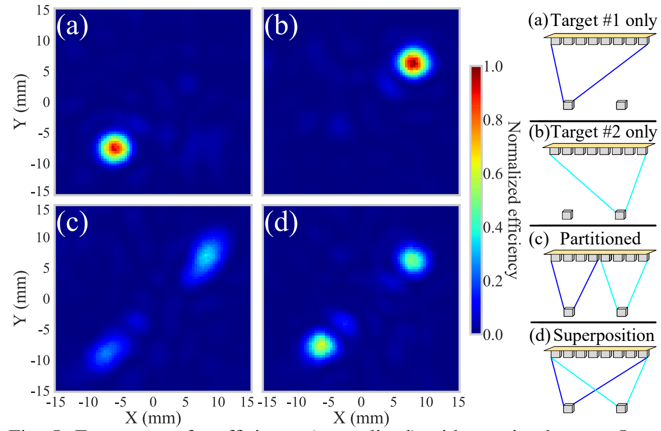

Fig. 5: Energy transfer efficiency (normalized) with two implants at 5 cm depth with separate and simultaneous time reversal. Illustrations demonstrating each setup are also shown. (a) Target #1 (-6 mm, -8 mm) only. (b) Target #2 (8 mm, 6 mm) only. (c) Partitioned array. (d) Superposition.

TABLE I: Efficiency (normalized to peak value) of separate and simultaneous time reversal measurements to 2 implants at different depths.

	Depth	Target 1	Target 2	Partitioned	Superposition
Implant 1	3 cm	1.0	0.009	0.34	0.41
Implant 2	4 cm	0.005	0.48	0.14	0.20

REFERENCES

[1] D. K. Piech, *et al.*, "A wireless millimetre-scale implantable neural stimulator with ultrasonically powered bidirectional communication," *Nature Biomed. Eng.*, vol. 4, no. 2, pp. 207–222, 2020.

[2] J. Charthad, *et al.*, "A mm-sized wireless implantable device for electrical stimulation of peripheral nerves," *IEEE Trans. Biomed. Circuits Syst.*, vol. 12, no. 2, pp. 257–270, 2018.

[3] S. F. Alamouti, *et al.*, "High throughput ultrasonic multi-implant readout using a machine-learning assisted cdma receiver," in *2020 42nd Annu. Int. Conf. IEEE Eng. Medicine Biol. Soc.*, 2020, pp. 3289–3292.

[4] J. Thimot and K. Shepard, "Bioelectronic devices: Wirelessly powered implants," *Nature Biomed. Eng.*, vol. 1, p. 0051, 03 2017.

[5] M. M. Ghanbari and R. Muller, "Optimizing volumetric efficiency and backscatter communication in biosensing ultrasonic implants," *IEEE Trans. Biomed. Biomed. Syst.*, pp. 1–1, 2020.

[6] D. Seo, *et al.*, "Ultrasonic beamforming system for interrogating multiple implantable sensors," in *2015 37th Annu. Int. Conf. IEEE Eng. Medicine and Biol. Soc.*, 2015, pp. 2673–2676.

[7] M. L. Wang, *et al.*, "Closed-loop ultrasonic power and communication with multiple miniaturized active implantable medical devices," in *2017 IEEE Int. Ultrasonics Symp.*, 2017, pp. 1–4.

[8] M. L. Wang, T. C. Chang, and A. Arbabian, "Ultrasonic implant localization for wireless power transfer: Active uplink and harmonic backscatter," in *2019 IEEE Int. Ultrasonics Symp.*, 2019, pp. 818–821.

[9] M. Meng and M. Kiani, "Self-image-guided ultrasonic wireless power transmission to millimeter-sized biomedical implants," in *2019 41st Annu. Int. Conf. IEEE Eng. Medicine Biol. Soc.*, 2019, pp. 364–367.

[10] M. Fink, "Time reversal of ultrasonic fields. i. basic principles," *IEEE trans. ultrasonics, ferroelectrics, and frequency control*, vol. 39, pp. 555–66, 02 1992.

[11] M. Fink, G. Montaldo, and M. Tanter, "Time-reversal acoustics in biomedical engineering." *J. Acoust. Soc. Amer.*, vol. 123, p. 3428, 06 2008.

[12] D. Arnaud, P. Roux, and M. Fink, "Robust acoustic time reversal with high-order multiple scattering," *Physical rev. lett.*, vol. 75, pp. 4206–4209, 01 1996.

[13] H. S. Gougheri, *et al.*, "A comprehensive study of ultrasound transducer characteristics in microscopic ultrasound neuromodulation," *IEEE Trans. Biomed. Circuits Syst.*, vol. 13, no. 5, pp. 835–847, 2019.

[14] R. J. Mailloux, *Phased Array Antenna Handbook*, 2nd ed. Boston: Artech House, 2005.

[15] T. C. Chang, M. Wang, and A. Arbabian, "Multi-access networking with wireless ultrasound-powered implants," in *2019 IEEE Biomed. Circuits Syst. Conf.* IEEE, 2019, pp. 1–4.